

PAPER • OPEN ACCESS

Studying the variation of the slip factor when trimming the impeller of centrifugal pumps

To cite this article: Kliment Klimentov *et al* 2023 *IOP Conf. Ser.: Earth Environ. Sci.* **1128** 012015

View the [article online](#) for updates and enhancements.

You may also like

- [A displacement-based method for evaluating the stability of a pile-stabilized slope](#)

Yang Yu, Pin Lu, Bo Shi *et al.*

- [Influences of Surface Topography on the Flying Performances of a Sub-3 nm Air Bearing Slider](#)

Wei Hua, Bo Liu, Shengkai Yu *et al.*

- [Correspondence between Layered Cell Structures and Slip Lines in Deformed Copper Single Crystals](#)

Yz Kawasaki



The Electrochemical Society
Advancing solid state & electrochemical science & technology

DISCOVER
how sustainability
intersects with
electrochemistry & solid
state science research



Studying the variation of the slip factor when trimming the impeller of centrifugal pumps

Kliment Klimentov^{1,2}, Desislava Nikolova¹, Gencho Popov³ and Boris Kostov¹

¹ Department of Heat, Hydraulics and Environmental Engineering, University of Ruse, Ruse 7017, Bulgaria

² kklimentov@uni-ruse.bg

Abstract.

It is well-known that one of the reasons for reducing the head of a centrifugal pump, when trimming its impeller, is the reduction of the slip factor. There are various methods used to determine it, but there is lack of information on whether they are applicable in case that a pump with a trimmed impeller operates. In the present work, a comparative experimental study concerning the applicability of some of the methods used to determine the slip factor, on two centrifugal pumps with different specific speed of rotation, is performed. Based on the experimental data, CFD models of the impellers of the two pumps have been validated and a numerical simulation study concerning the change of the slip factor during trimming, has also been performed. The impact of the rate of impeller trimming on the the slip factor variation has also been established. Based on the results found, concerning the performed numerical study, equations describing the relationship between the slip factor and the rate of trimming of the studied pumps are obtained.

1. Introduction

It is known that the theoretical head H_{th} of centrifugal pumps is less than the one $H_{th\infty}$ in case of an infinite number of blades of the impeller, that is determined by applying Euler's equation:

$$H_{th\infty} = \frac{u_2 c_{2u\infty} - u_1 c_{1u\infty}}{g}, \quad (1)$$

where $u_1 = (\pi n D_1)/60$ is the peripheral velocity at the leading (input) edge of the impeller blade; $u_2 = (\pi n D_2)/60$ - the peripheral velocity at the trailing (output) edge of the impeller blade; n - speed of rotation, given in (min^{-1}) ; D_1 and D_2 - the diameters at the leading and trailing edges of the impeller blade, respectively, given in figure 1; $c_{1u\infty}$ and $c_{2u\infty}$ - peripheral components of the absolute velocity at the leading and trailing edges of the impeller blade, respectively; g - the gravity acceleration.

Usually, it is assumed that $c_{1u\infty} = 0$ (radial inflow) and equation (1) may be transformed and presented into the following form:

$$H_{\text{th}\infty} = \frac{u_2 c_{2u\infty}}{g}. \quad (2)$$

The decrease in H_{th} compared to $H_{\text{th}\infty}$ is due to the impact of various factors, the most important of which, according to Gulich, are the following ones [1]:

- the difference between the velocities acting on the abdominal and posterior blade sides;
- Coriolis forces acting in a direction opposite to the peripheral velocity, which leads to the occurring of secondary flows in the interblade impeller channels. These flows are the main reason for varying the flow angle at the impeller output from β_{2b} to β'_2 , as given in figure 2.
- a variation in the shape of the relative flow streamlines near the impeller output.

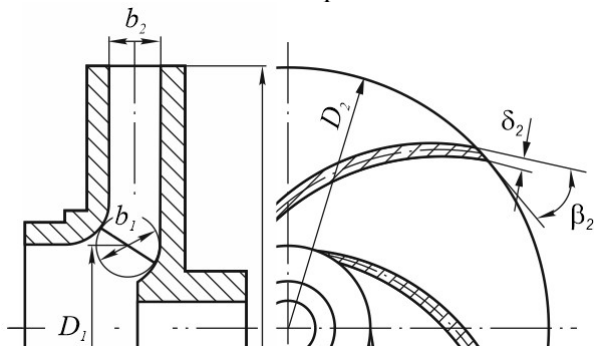


Figure 1. Specific sizes of the impeller geometry of a centrifugal pump.

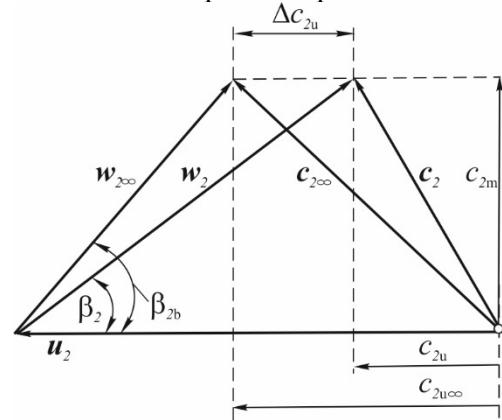


Figure 2. Velocity triangles just before the impeller output of a centrifugal pump.

The impact of the previously mentioned factors on the theoretical impeller head is to be determined by introducing the slip factor. According to the different literature source various definitions of slip factor can be seen, but two of them are recognized as main ones. According to one of these two definitions, mainly used in the US, the slip factor is determined by the equation [2]:

$$\mu_{\text{US}} = 1 - \frac{\Delta c_{2u}}{u_2}, \quad (3)$$

where Δc_{2u} is used to indicate the difference between the absolute velocities c_2 and $c_{2\infty}$ at the impeller output, as given in figure 2.

The second definition, mainly used in Europe, is presented by the following equation [2]:

$$\mu_{\text{EU}} = \frac{c_{2u}}{c_{2u\infty}} = 1 - \frac{\Delta c_{2u}}{c_{2u\infty}}, \quad (4)$$

The relationship between μ_{US} and μ_{EU} may be presented as follows:

$$\mu_{\text{EU}} = 1 - \frac{u_2}{c_{2u\infty}} (1 - \mu_{\text{US}}), \quad (5)$$

where: β_{2b} is the angle of the impeller blades at diameter D_2 , given in fig. 2; c_{2m} is the meridian projection of the absolute velocity acting in the interblade impeller channel, at diameter D_2 . It may be determined by applying the equation below:

$$c_{2m} = k_2 \frac{Q_{\text{imp}}}{\pi b_2 D_2}, \quad (6)$$

where Q_{imp} is the volume flow rate of the water flow passing through the impeller channels; b_2 - the width of the interblade channel at diameter D_2 , given in figure 1. The narrowing factor (coefficient) k_2 may be estimated by applying the following equation [1]:

$$k_2 = \left(1 - \frac{\delta_2 z}{\pi D_2 \sin \beta_{2b}} \right)^{-1}. \quad (7)$$

In equation (7) δ_2 is used to indicate the blade width at the impeller output, as given in figure 1, and z indicates the number of impeller blades.

In the present work, the definition according to equation (4) is adopted to determine the slip factor, since in this way it will represent the ratio between H_{th} and $H_{\text{th}\infty}$. The symbol μ will be used further in this work, considering that $\mu = \mu_{\text{EU}}$.

One of the methods used to obtain a permanent change of a pump system operating mode is by trimming the pump impeller. There are various empirical equations for predicting the pump head curve when operating with a trimmed impeller. The most commonly used (in nowadays) of them are presented in [1].

In [3], the impact of the rate of impeller trimming on the performance of two partial emission pumps has been studied. An energy balance is performed and some equations used to predict the hydraulic, volumetric and mechanical pump coefficients of efficiency when operating with trimmed impellers, are obtained. The impact of the rate of trimming on the slip factor has also been analyzed, and thus empirical equations describing the studied hydraulic relationships are proposed.

The authors in [4] present a numerical study of the effect of shroud trimming on the performance of pumps with low and medium specific speeds of rotation ($n_q = 10 \text{ min}^{-1}$ и $n_q = 24 \text{ min}^{-1}$). It is found that using Shear stress transport turbulence model provides results that are closer to the experimental ones, compared to the using of RNG $k - \varepsilon$ turbulent model. In addition to that, still in [4], some data concerning the impact of the rate of trimming on the distribution of the pressure coefficient, as well as on the forces acting on the impeller, is given. In [5] it is studied the impact of the pump impeller rate of trimming on the pressure fluctuation and radial force of two-stage self-priming centrifugal pump. For performing the numerical simulation Shear stress transport turbulent model is used.

Energy losses and radial force, came as a result of trimming the impeller of a double-suction centrifugal pump, are studied in [6]. It is found that the empirical equations used to predetermine the pump head do not provide a good overlapping with the experimental data, mainly due to an increase in the hydraulic losses in the volute, obtained after trimming. This is highly pronounced (can be clearly seen) in overloaded operating modes.

In [7] a numerical studying of trailing edge flow in centrifugal pump impellers, is performed. The impact of the shape of the trailing (outgoing) edge and the angle of the vane at the impeller exit on the slip factor is determined. To perform the numerical simulations 2D Reynolds-averaged Navier–Stokes equations and detached eddy simulations, are used.

The authors in [8], [9] and [10], have presented results of numerical and experimental studies on the impact of different centrifugal pump impeller geometrical parameters on the slip factor. In [8] numerical results, concerning the impact of the number of impeller blades on the slip factor, are presented. For solving Reynolds-averaged Navier–Stokes equations the $k - \varepsilon$ turbulent model is used. The results of a similar study are published in [9], where, in addition to the impact of the number of blades, the impact of the outgoing angle of the blades on the slip factor is studied, as for this aim CFD has been used.

Experimental and numerical studying of the slip factor reduction in centrifugal slurry pump are presented in [10]. The slip factor on the impeller channel is calculated on the tangential and the blade height directions. It deduced that the value of the slip factor reduces from the suction side to the pressure side on the channel [10].

Summarizing literature review, it is clear that there is a lack of sufficient data concerning the impact of the rate of impeller trimming on the slip factor in single-stage pumps with volute casing. Moreover, it is not clear how applicable in terms of accuracy the well-known equations for determining the slip factor are valid in the case of impeller trimming. The purpose of the present work is to obtain numerical results concerning the impact of the rate of impeller trimming on the slip factor for centrifugal pumps with volute casing and different specific speeds of rotation.

2. Methods to determine the slip factor

In this section of this work some of the known methods for determining the slip factor, published in different literature sources, are reviewed.

2.1. Stodola equation.

One of the earliest and simplest expressions for determining the slip factor has been obtained by A. Stodola (1927). His hypothesis for estimating the slip factor is presented in a book by S.L. Dixon [11], as well as in the articles of , T.W. von Backström [12], [13] and [14], Harrison H. M at al. [15]. As a main reason of flow deviation in a centrifugal pump impellers it is (mainly) considered to be the so-called relative axial eddy, which leads to the decrease in the velocity c_{2u} at the impeller output. The equation proposed by Stodola, used to determine the slip factor, is presented as follows [15]:

$$\mu_{\text{Stodola}} = \frac{\frac{\pi}{z} u_2 \sin \beta_{2b}}{u_2 - c_{2m} \operatorname{ctg} \beta_{2b}}. \quad (8)$$

2.2. Stanitz equation.

Stanitz [11], [15] proposes an equation for determining the slip factor, obtained after a theoretical study of eight centrifugal and diagonal compressors impellers, with a vane exit angle from 0 to 45 degrees. The author suggests that the slip velocity Δc_{2u} is independent of the blade angle β_{2b} and depends only on the step of the blades. The equation proposed by Stanitz, in respect to equation (3), may be presented as follows [15]:

$$\mu_{\text{US}} = 1 - 0.63 \frac{\pi}{z}. \quad (9)$$

Using equation (5) relating μ_{US} and μ_{EU} , equation (9) may be presented into the following way:

$$\mu_{\text{Stanitz}} = 1 - \frac{0.63 \frac{\pi}{z}}{1 - \frac{c_{2m}}{u_2 \tan \beta_{2b}}}. \quad (10)$$

2.3. Pfleiderer equation.

To estimate the theoretical pump head at finite number of blades, the equation of Pfleiderer is often used [16]:

$$H_{\text{th}} = \frac{1}{1 + p} H_{\text{th}\infty}. \quad (11)$$

To fix the head value Pfleiderer implements a correction factor p , used to indicate the finite number of the blades, that is based on the following statements:

- the load per unit length of the blade is constant throughout the whole blade surface;
- near the blade exit pressure and velocity are unevenly distributed.

This Pfleiderer correction is not a slip factor, but a head correction due to the finite number of blades. It can be related to the slip factor and presented as follows:

$$\mu_{\text{Pfleiderer}} = \frac{1}{1+p}. \quad (12)$$

The coefficient p in equation (12) may be estimated as follows [16]:

$$p = 2 \frac{(0.55 \div 0.68) + 0.6 \sin \beta_{2b}}{z} \left[1 - \left(\frac{D_1}{D_2} \right)^2 \right]^{-1}. \quad (13)$$

2.4. Wiesner equation.

In [1], a modified Wiesner equation for determining the slip factor is proposed:

$$\mu_{\text{US}} = 0.98 \left(1 - \frac{\sqrt{\sin \beta_{2b}}}{z^{0.7}} \right), \quad (14)$$

at $\frac{D_1}{D_2} \leq \varepsilon_{\text{Lim}}$ and

$$\mu_{\text{US}} = 0.98 \left(1 - \frac{\sqrt{\sin \beta_{2b}}}{z^{0.7}} \right) \left[1 - \left(\frac{\frac{D_1}{D_2} - \varepsilon_{\text{Lim}}}{1 - \varepsilon_{\text{Lim}}} \right)^3 \right], \quad (15)$$

at $\frac{D_1}{D_2} > \varepsilon_{\text{Lim}}$, where $\varepsilon_{\text{Lim}} = e^{\left(-8.16 \frac{\sin \beta_{2b}}{z} \right)}$.

By taking into account equation (5), in case that $\frac{D_1}{D_2} \leq \varepsilon_{\text{Lim}}$, equation (15) may be presented:

$$\mu_{\text{Wiesner}} = 1 - \frac{u_2}{c_{2u\infty}} \left[1 - 0.98 \left(1 - \frac{\sqrt{\sin \beta_{2b}}}{z^{0.7}} \right) \right]. \quad (16)$$

2.5. Backström equation.

An interesting approach for estimating the slip factor is presented in some papers of T. W. von Backström [12], [13], [14]. He states that he has developed a method that combines the well-known methods for predicting the slip factor of a centrifugal impeller of Stodola, Stanitz, Wiesner in a common equation. He presents this method as applicable in predicting the slip coefficient for radial and backward-facing impellers. The analytical method he developed derives the slip velocity in terms of a single relative eddy - SRE. This eddy is centered on the axis of the impeller instead of the usual multiple (one per a blade channel) eddies, adopted by Stodola. He introduced the concept of "blade stiffness", which represents the ratio between the blade length l and $t_2 = (\pi D_2)/z$ at the impeller output. The parameter l/t_2 is considered as a main variable, determining the slip factor.

To determine the slip factor, it is recommended to use the following equation:

$$\mu_{\text{US}} = 1 - \frac{1}{1 + F \frac{l}{t_2}}. \quad (17)$$

The coefficient F (impact factor of blade stiffness in applying the SRE method) depends on the angle β_{2b} and z , and may be determined by applying the equation below [12], [13], [14]:

$$F = 2 + \left(2.71 + \frac{\pi}{z} \sin \beta_{2b} \right) \sin \beta_{2b}. \quad (18)$$

By taking into account equation (5), equation (17) is transformed into the following way:

$$\mu_{\text{EU}} = 1 - \frac{u_2}{c_{2u\infty}} \frac{1}{1 + F \frac{l}{t_2}}. \quad (19)$$

3. Determining experimentally the slip factor of centrifugal pumps of the type 6E32 and 12E20

3.1. Object of study

Objects of research (study) in this paper are two centrifugal pumps manufactured by Vipom Ltd., Vidin (Bulgaria). Data concerning their main indicators and geometric parameters is presented in table 1. The specific speed of rotation of the two pumps is estimated by applying equations (20) and (21):

$$n_q = n_n Q_n^{0.5} H_n^{-0.75} \quad (20)$$

and

$$n_s = 3.65 n_n Q_n^{0.5} H_n^{-0.75}, \quad (21)$$

where n_n , Q_n and H_n are the nominal values of the speed of rotation, volume flow rate and head of the studied pumps, respectively.

Table 1. Main pump indicators and geometric sizes of the studied pumps.

	n_n (min ⁻¹)	Q_n (dm ³ s ⁻¹)	H_n (mH ₂ O)	n_q (min ⁻¹)	n_s (min ⁻¹)	z	D_2 (mm)	b_2 (mm)	δ_2 (mm)	β_{2b} (deg)
6E32	2900	6	32	16.7	60.9	6	166	5.7	4	25.66
12E20	2900	12	20	33.6	122.6	7	142	14.3	4	24.19

3.2. Analytical and experimental determination of the slip factor for the two studied pumps.

For the experimental determination of the slip factor, data obtained in the "Hydro and Pneumatic Engineering" laboratory of the "Angel Kanchev" University of Ruse, is used. To perform the experiments a specialized laboratory test system, presented in [17] and [18], has been used. A scheme of the system used to determine the volume and mechanical losses in the studied pumps is presented in figure 3. The energy tests are also performed by using the same system.

When determining volume losses and disc friction losses, the impeller - position 13, of the studied pump has been preliminary filled with wax. Volume losses through the front seal of the pump are determined after measuring the mass flow rate of water through the seal using the scale - position 10, and a stopwatch. Water circulation is provided by using an auxiliary pump unit - position 14. Bearing friction torque and disk friction torque are determined using a dial scale - position 1. The complete methodology for establishing the pumps power balance is presented in [17] and [18].

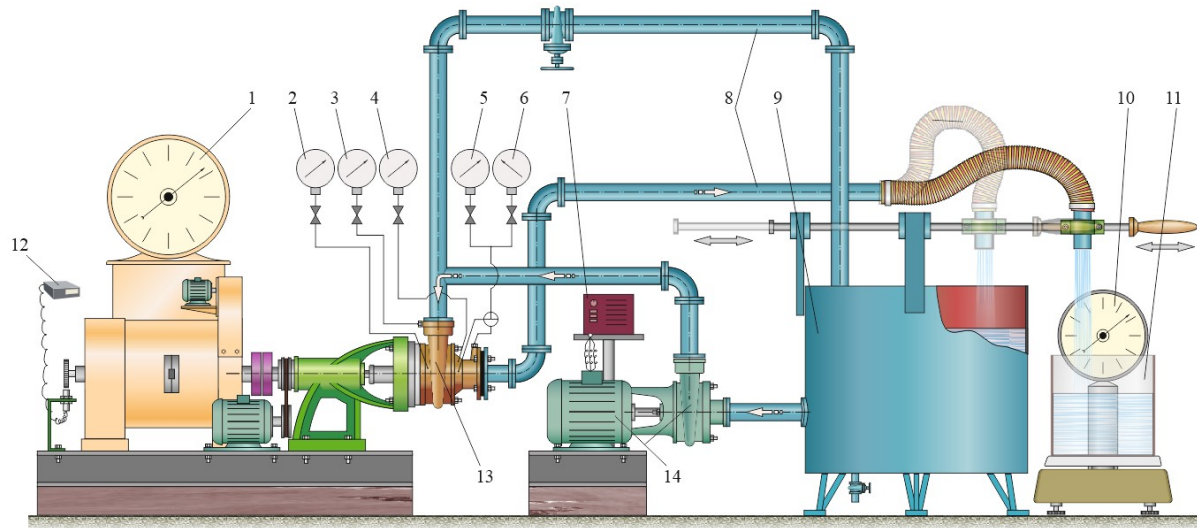


Figure 3. Test rig for power balance investigation of centrifugal pumps. 1- dial scale for torque measurement of a motor; 2, 3, 4, 5, 6- pressure gauges; 7- variable frequency drive; 8-pipes; 9- open tank; 10-dial scale for mass flow rate measurement; 11-open tank;12-tachometer; 13-tested pump; 14- auxiliary pump.

For the analytical determination of the slip factor, the equations previously discussed (in point 2), are used. The results obtained for the two studied pumps are presented graphically in figures 4 and 5.

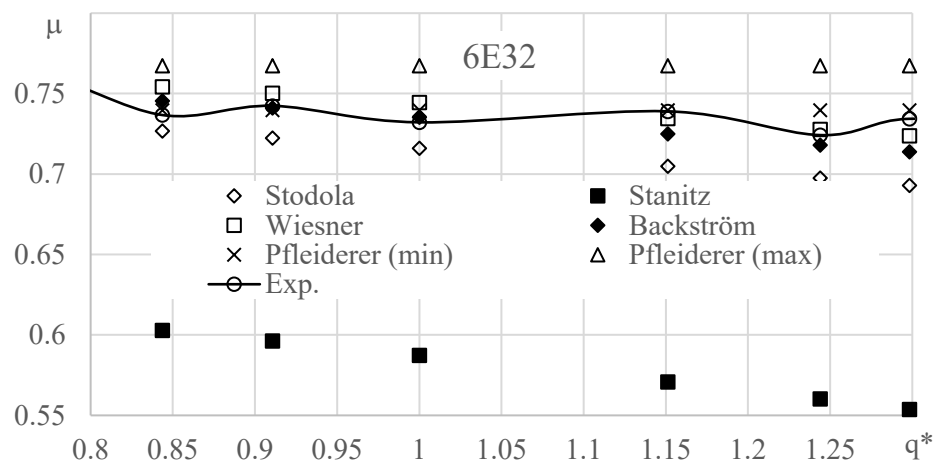


Figure 4.
Equations of
the type
 $\mu = f(q^*)$ for
pump 6E32,
obtained
experimentally
and
analytically.

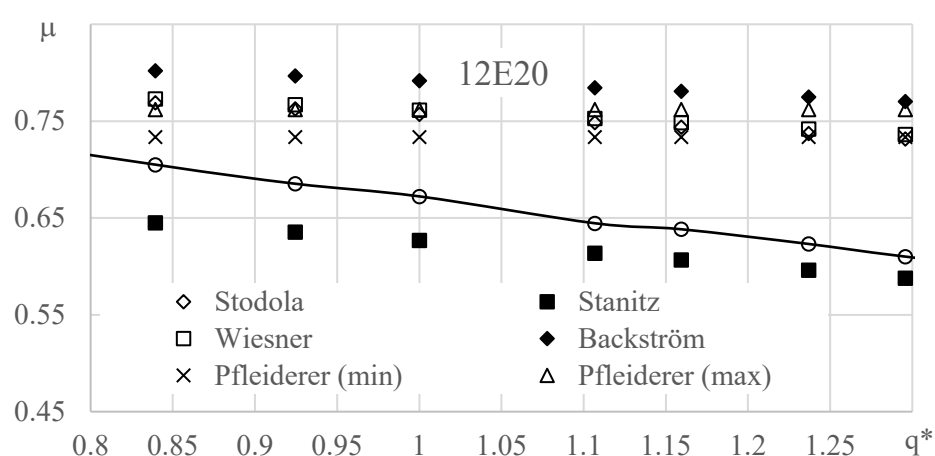


Figure 5.
Equations of
the type
 $\mu = f(q^*)$ for
pump 12E20,
obtained
experimentally
and
analytically.

Values, concerning “Pfleiderer (min)” are obtained by using equation (12), where the coefficient $p = 2 \frac{0.68 + 0.6 \sin \beta_{2b}}{z} \left[1 - \left(\frac{D_1}{D_2} \right)^2 \right]^{-1}$, while “Pfleiderer (max)”- $p = 2 \frac{0.55 + 0.6 \sin \beta_{2b}}{z} \left[1 - \left(\frac{D_1}{D_2} \right)^2 \right]^{-1}$.

Results that are similar to the experimental data, for pump 6E32, are obtained by applying the equations of Wiesner, Pfleiderer (min), and Backström. For the second studied pump (12E20), the closest (most similar) to the experimental data are the results obtained by applying the equation of Stanitz, where a trend for a more distinct decrease of μ with an increase in q^* , is indicated. The same trend is observed in the results obtained by applying Stodola equation for pump 6E32. According to the other applied equations, relatively close constant values of μ , close to 0.75, are obtained. In order to determine the rate of validation concerning the the studied equations, applied in case of trimming pump impellers, some numerical simulation studies using the ANSYS CFX subroutine, are performed.

4. CFD modeling the slip factor in case of trimming centrifugal pump impellers

4.1. Validation of CFD models of the impellers of the studied pumps

According to Gulich [1] in the relative volume flow rate range (RFR) $0.7 < q^* < 1.1$ ($q^* = Q / Q_n$) it is possible to perform numerical study of the impeller only, since in this range there is slight interaction between the impeller and the corresponding booster element installed at its output.

In the present work, geometric models are developed and computational meshes of the impellers of the two studied pumps are generated, as for this aim ANSYS has been used. In order to minimize the impact of the number of NE elements of the mesh on the results, 4 meshes with different numbers of elements are generated concerning the impeller of the 12E20 pump. The meshes are unstructured, with a core of tetrahedral elements and with varying numbers of prismatic layers on the solid walls of the impellers. More detailed information concerning the computational meshes is presented in table 2.

Table 2. Data concerning the computational meshes of the impeller of a pump 12E20.

	MS (mm)	MFS (mm)	FLT (mm)	GR	N	NE.10 ⁻⁶	Ψ _{th}	Ψ _p
Mesh1	1.1	1.1	0.0005	1.5	19	4.303	1.068	0.733
Mesh2	1.0	1.0	0.0005	1.5	18	5.448	1.065	0.733
Mesh3	0.8	0.8	0.0005	1.5	18	9.358	1.056	0.732
Mesh4	0.6	0.6	0.0005	1.5	17	19.958	1.046	0.730

Table 2 content information about the values of the maximum element size (*MS*) of the volumetric mesh, maximum face size (*MFS*), first layer thickness (*FLT*), growth rate (*GR*) - growth factor of the height of the prismatic layers, number of prismatic layers *N*, number of elements of the network (*NE*), as well as the values of the coefficients of theoretical Ψ_{th} (*THC*) and static Ψ_p (*SHC*) head of the studied pump impeller. The last two parameters are to be determined by applying the following equations:

$$\Psi_{th} = 2gH_{th} / u_2^2 \quad (22)$$

and

$$\Psi_p = 2gH_p / u_2^2, \quad (23)$$

where $H_p = (p_{out} - p_{in}) / (\rho g)$ is the impeller static head; p_{in} - the static head in front of the impeller input; p_{out} - the static head after the impeller output; ρ - water density. The values of p_{in} , p_{out} and H_{th} are obtained after performing numerical simulations in ANSYS CFX. The flows in the impellers are modeled using Rotating Frames of Reference applicable to rotating fluid machinery applications,

such as pump impeller or turbine blade problems. The turbulent model Shear Stress Transport (SST) is used.

Analyzing the data in table 2, it can be clearly seen that when the number of mesh elements increases from 9.358 million to 19.958 million, (more than twice) the theoretical head coefficient decreases from 1.056 to 1.046, which means a change of 0.96%. At the same time, the coefficient of static head decreased from 0.732 to 0.730, which means a change of 0.24%. These are the reasons so to select Mesh4 for performing the numerical experiments concerning the two studied pump impellers.

In figures 6 and 7 the relationships of the types $\Psi_{th} = f(q^*)$ and $\Psi_p = f(q^*)$, obtained both – experimentally and by using ANSYS CFX, are presented. In addition to that it is also presented the relative deviation/error (RE) relationships of Ψ_{th} and Ψ_p , estimated by applying the equation below:

$$\Delta = \frac{\Psi(\text{Exp.}) - \Psi(\text{CFX})}{\Psi(\text{Exp.})} 100\%. \quad (24)$$

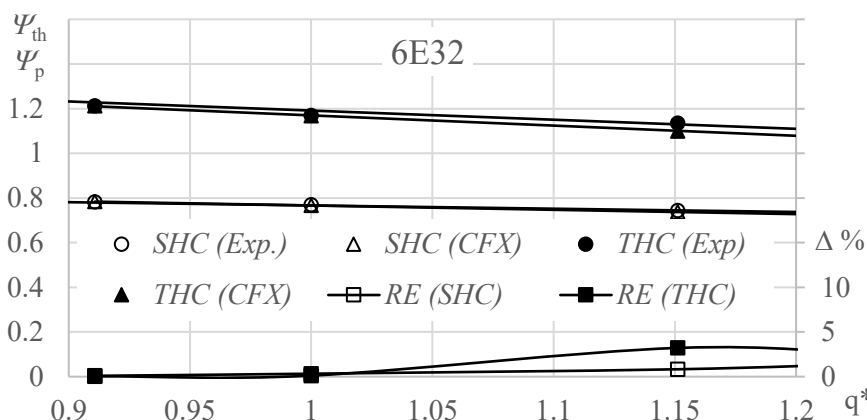


Figure 6.
Relationships of the type $\Psi_{th} = f(q^*)$, $\Psi_p = f(q^*)$ and $\Delta = f(q^*)$ for pump 6E32.

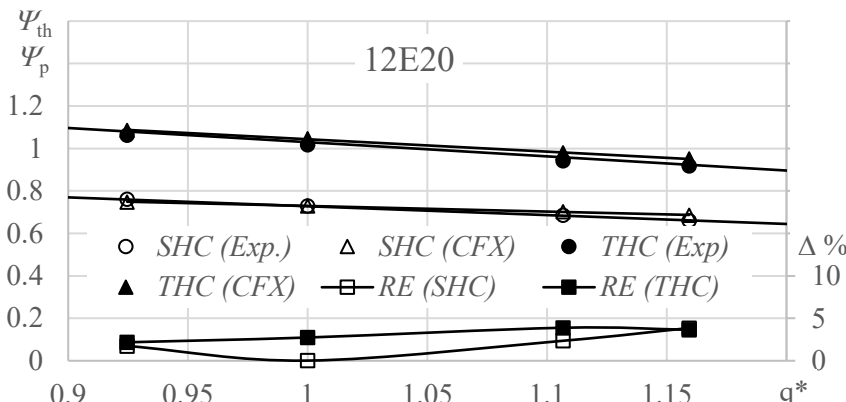


Figure 7.
Relationships of the type $\Psi_{th} = f(q^*)$, $\Psi_p = f(q^*)$ and $\Delta = f(q^*)$ for pump 12E20.

It can be seen from the figures that the maximum value of RE in the studied range of relative flow rates is less than 5%, which is less than the permissible value of 10% stated in [1] for performing this kind of research.

4.2. Results of numerical studies of pumps 6E32 and 12E20 when operating with trimmed impellers.
In the manufacturer catalog of the studied pumps, it is specified that the 6E32 pump is available with two additional impellers with outlet diameters of 152 mm and 142 mm. The 12E20 pump is available with one additional impeller with a diameter of 130 mm. For the purpose of this study, two models of impellers are developed for the two studied pumps. Information about some geometric parameters of the models is presented in table 3.

Table 3. Sizes of the models of the studied pump impellers.

	D_2 (mm)	b_2 (mm)	δ_2 (mm)	β_{2b} (deg)
6E32	166	5.7	4	25.66
6E32	152	5.7	4	30.19
6E32	142	5.7	4	32.82
12E20	142	14.3	4	24.19
12E20	136	14.562	4	21.43
12E20	130	14.826	4	19.23

Simulation calculations are performed for the six studied models. The calculation mesh - Mesh4, containing: a turbulent model SST, turbulent intensity at the inlet of the impellers – 10% and max residual of the equations at the end of the calculations – $5 \cdot 10^{-4}$, is used. The arithmetic mean value of the dimensionless distance, directed normal to the walls, to the first calculation point of the blade surface, is $y^+ < 1$ for all models, in each calculation mode.

In figures 8 and 9 it is presented (graphically) the function $\mu = f(D_2^*)$, at different values of q^* . The symbol D_2^* is used to indicate the relative diameter of the pump trimmed impellers, determined by applying the following equation:

$$D_2^* = D_{2,trim} / D_2 . \quad (25)$$

where $D_{2,trim}$ is the diameter of the trimmed pump impeller.

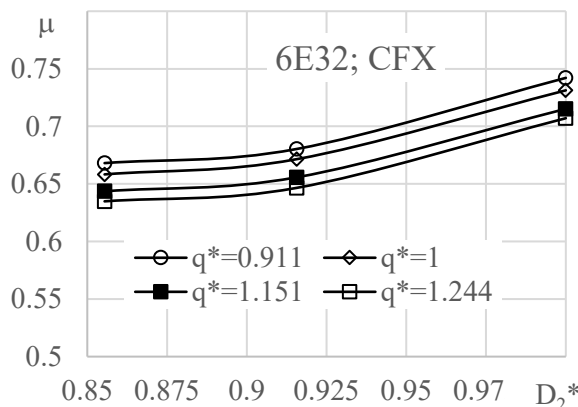


Figure 8. Relationships of the type $\mu = f(D_2^*)$ for pump 6E32, at different values q^*

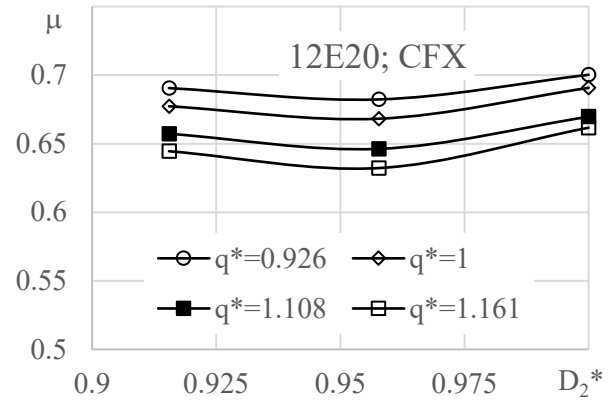


Figure 9. Relationships of the type $\mu = f(D_2^*)$ for pump 12E20, at different values of q^*

It is noteworthy that for the impeller of the 6E32 pump, a visible decrease of μ with a decrease of D_2^* by nearly 10% at $D_2^* = 0.855$, while for the impeller of the 12E20 the slip factor practically does not change.

In figures 10 and 11 it is presented graphically the relationships of the type $\mu = f(D_2^*)$, at $q^*=1$, obtained by applying the previously discussed equation, as well as ANSYS CFX. For the 6E32 pump impeller, good corresponding (overlapping) is observed between the results obtained using ANSYS CFX and applying the Stodola equation. In the case when studying the impeller of a 12E20 pump, no coincidence of the results of the numerical simulations with those obtained by any of the proposed equations is observed. One of the likely reasons for the different trends in the two studied impellers is the various change in the angle β_{2b} . In case of studying the impeller of the 6E32 pump, the angle β_{2b}

increases as the outer diameter decreases, while in the case of the 12E20 pump, it is the opposite (decreases). Because of that the velocity $c_{2u\infty}$ is going to decrease less for pump 6E32 than for pump 12E20, which leads to a more intensive reduction of the slip factor $\left(\mu = 1 - \frac{\Delta c_{2u}}{c_{2u\infty}} = \frac{c_{2u}}{c_{2u\infty}}\right)$. This can be clearly seen in figure 12, where the relationships of the type $c_{2u\infty}^* = f(D_2^*)$ for the two studied pumps are graphically presented. The values of $c_{2u\infty}$ (indicated as $c_{2u,\text{inf}}$) are obtained by applying the following equation:

$$c_{2u\infty}^* = c_{2u\infty,\text{trim}} / c_{2u\infty,0}. \quad (26)$$

In equation (26) the symbol $c_{2u\infty,\text{trim}}$ is used to indicate the velocity in case of a trimmed pump impeller, and $c_{2u\infty,0}$ is used for the case of normal (untrimmed) pump impeller.

In figure 13 some relationships of the type $\mu^* = f(D_2^*)$, for the two studied pumps, where $\mu^* = \mu_0 / \mu_i$, are presented. The symbol μ_0 is used to indicate the value of the slip factor when pumps operate with normal (untrimmed) impellers, while μ_i is used in case of trimmed ones. The data used for plotting the curves in figure 13 are preliminary processed in MATLAB and the relationships of the type $\mu^* = f(D_2^*)$ are approximated by equations of the type:

$$\mu^* = aD_2^{*2} + c. \quad (27)$$

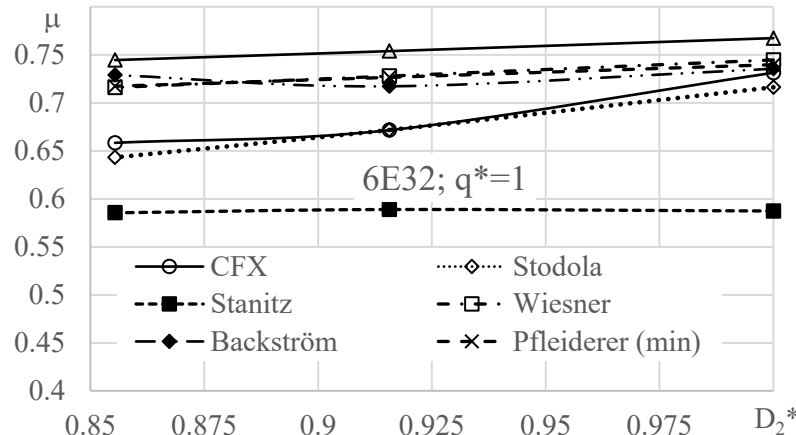


Figure 10. Relationships of the type $\mu = f(D_2^*)$ for pump 6E32, at $q^*=1$, obtained by applying different equations, as well as ANSYS CFX

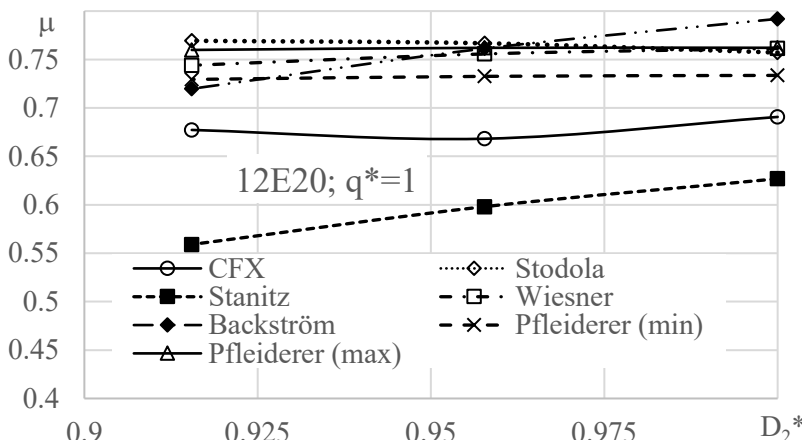


Figure 11. Relationship of the type $\mu = f(D_2^*)$ for pump 12E20, at $q^*=1$, obtained by applying different equations, as well as ANSYS CFX

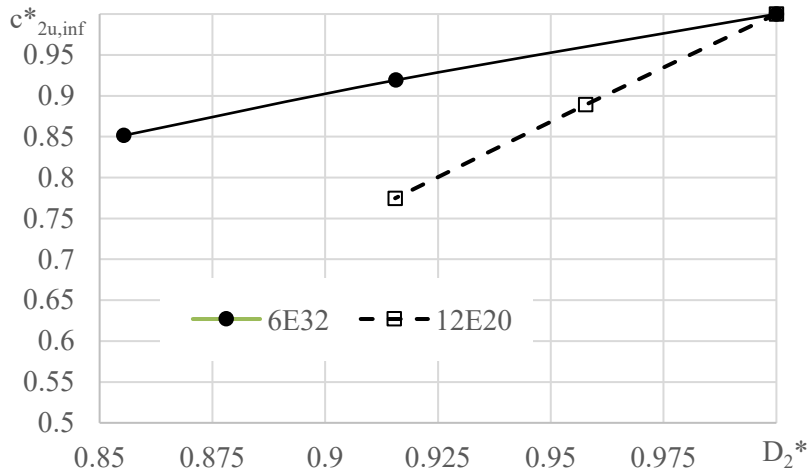


Figure 12. Relative change of the velocity $c_{2u,\infty}^*$ depending on D_2^*

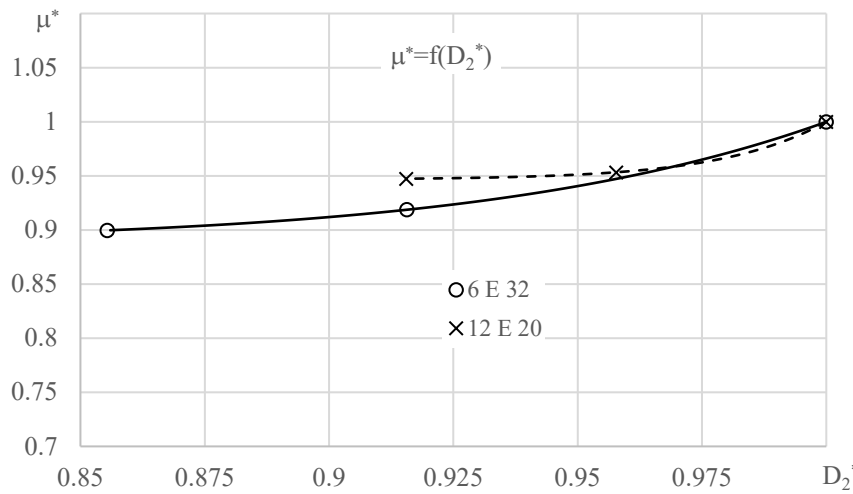


Figure 13. Relationships of the type $\mu^* = f(D_2^*)$, obtained for the two studied pumps.

The values of the coefficients in eq. (27) are set to be: for pump 6E32 - $a = 0.1111$, $b = 14.9$, $c = 0.8888$, coefficient of determination $R^2 = 1$, and for pump 12E20 - $a = 0.0534$, $b = 48.0$, $c = 0.9466$, coefficient of determination $R^2 = 1$. The solid and dashed lines in figure 10 are obtained (plotted) by applying eq. (27) for the two studied pumps.

Analyzing the data, presented in figure 10, it is clear that in the range $D_2^* = 0.95 \div 1$, μ^* decreases with same intensity for both pumps, which continues up to $\mu^* = 0.95$, and after that it doesn't variate anymore concerning pump 12E20. For the pump 6E32 the decrease is 10% compared with its initial value at $D_2^* = 0.855$.

5. Conclusion

The paper presents the results of an experimental, analytical and numerical study of the slip factor for two centrifugal pumps with different specific speeds of rotation. The most important results and conclusions of the work are the following ones:

- Experimental results have been obtained for the theoretical and potential head of two centrifugal pumps with different specific speeds, when operating with untrimmed impellers;

- CFD models of the impellers of the studied pumps are established. The relative deviation from the numerical results for theoretical and potential heads is below 5%, when operating with untrimmed impellers and in the range $q^* = 0.92 \div 1.15$;
- Numerical results are obtained, using CFD modeling, for the slip factor of the two pumps, when operating with untrimmed and trimmed impellers. The results are compared with data obtained by applying well-known hydraulic equations. It is found that the best match of the slip factor when operating with a trimmed impeller is obtained between the numerical results for the 6E32 pump and the data obtained by the Stodola equation;
- The impact of impeller trimming on the slip factor variation is developed and some hydraulic relationships of the type $\mu^* = f(D_2^*)$ are obtained. These relationships are presented by equations of the type $\mu^* = aD_2^{*2} + c$, whose coefficients are determined for pumps 6E32 and 12E20.

Acknowledgments

This current paper presents the results of working on project No. 2022 - AIF - 03, funded by the Research Fund of the University of Ruse.

References

- [1] GÜLICH J Fr 2020 *Centrifugal Pumps* Fourth Edition, Springer-Villeneuve, Switzerland
- [2] Chen B, Song B, Tu B, Zhang Y, Li X, Li Z and Zhu Z 2021 Effect of Rotation Speed and Flow Rate on Slip Factor in a Centrifugal Pump *Shock and Vibration* **2021**
- [3] Li WG 2020 Affinity laws for impellers trimmed in two partial emission pumps with very low specific speed *Journal of Mechanical Engineering Science* **0(0)** pp 1-19
- [4] Shadab M, Karimipour M, Najafi A F, Paydar R and Nourbakhsh A 2022 Effect of impeller shroud trimming on the hydraulic performance of centrifugal pumps with low and medium specific speeds *Engineering Applications of Computational Fluid Mechanics* **16(1)** pp 514-535
- [5] Wang K, Zhang Z, Jiang L, Liu H and Li Y 2017 Effects of impeller trim on performance of two-stage self-priming centrifugal pump *Advances in Mechanical Engineering* **9(2)** pp 1-11
- [6] Deng Q, Pei J, Wang W, Lin B, Zhang C and Zhao J 2021 Energy Loss and Radial Force Variation Caused by Impeller Trimming in a Double-Suction Centrifugal Pump *Entropy* **2021, 23, 1228** pp 1-19
- [7] Litfin O and Delgado A 2019 *Numerical Investigation of Trailing Edge Flow in Centrifugal Pump Impellers* Proceedings of 13th European Conference on Turbomachinery Fluid dynamics & Thermodynamics ETC13 April 8-12, 2019; Lausanne, Switzerland
- [8] Khalafallah M, Elsheshtawy H, Ahmed AN M and El-Rahman A I A 2015 Flow simulation in radial pump impellers and evaluation of slip factor *Journal of power and energy* **0(0)** pp 1-10
- [9] Elsheshtawy H A 2012 *Numerical Study of Slip Factor in Centrifugal Pumps and Study Factors Affecting its Performance* Proceedings of 2012 International Conference on Mechanical Engineering and Material Science (MEMS 2012)
- [10] Abdolahnejad E, Moghimi M and Derakhshan S 2021 Experimental and numerical investigation of slip factor reduction in centrifugal slurry pump *Journal of the Brazilian Society of Mechanical Sciences and Engineering* **(2021) 43:179** pp1-14
- [11] Dixon S.L, Hall C.A. 2010 *Fluid Mechanics, Thermodynamics of Turbomachinery* Sixth edition Butterworth-Heinemann Linacre House, Jordan Hill, Oxford
- [12] Backström T W 2006 A Unified Correlation for Slip Factor in Centrifugal Impellers *Journal of Turbomachinery* **128/9**
- [13] Backström T W 2007 Relative-eddy induced slip in centrifugal impellers for engineering students R&D *Journal of the South African Institution of Mechanical Engineering* **23(1)** pp

21–27

- [14] Backström T W 2019 Factor Prediction for Impellers with Straight, Back-swept Blades *R&D Journal of the South African Institution of Mechanical Engineering* **35** pp 55–63
- [15] Harrison H M, Nicole L, Key N 2021 A New Approach to Modeling Slip and Work Input for Centrifugal Compressors *Journal of Engineering for Gas Turbines and Power* **143/021013-1**
- [16] Pfleiderer C 1955 *Die Kreiselpumpen für Flüssigkeiten und Gase* Springer-Verlag, Berlin
- [17] Klimentov K 2006 Methodologies for balance research of centrifugal pumps operating with water-air blends *Energetica* **4** pp 55-59.
- [18] Klimentov K 2010 *Investigation of centrifugal pumps performance with air-water two-phase flow* PHD Thesys, University of Ruse